FINAL REPORT

DE-FG02-05ER15730

Atomically dispersed supported metal species as catalysts for alcohol conversion, and hydrogen and chemicals production

PI: Maria Flytzani-Stephanopoulos[1]
CO PI: E. Charles. H. Sykes[2]
[1]Department of Chemical and Biological Engineering,
Tufts University, Medford, MA
[2]Department of Chemistry,
Tufts University, Medford, MA

Abstract

Supported single metal atoms are a new class of catalyst in which precious metals can be used at the ultimate limit of atom efficiency. While great strides have been made in demonstrating the potential of single-atom catalysts for many industrial reactions, there remains much debate in the literature over the nature of the active sites and the reaction mechanisms. The major goal of this project was to elucidate how atomic dispersions of metals on oxide supports enable catalytic reactions and how to stabilize such active sites for practical catalyst development. This is particularly important for the reactions of interest to fuel reforming for hydrogen generation in which atomically-dispersed metal ions on various oxide surfaces have been identified as the active sites. Working with trace amounts of precious metals is both fundamentally intriguing and of great practical interest in our continual search for low-cost, efficient and stable catalysts for the conversion of fuels to hydrogen under highly demanding operating conditions. A second major goal of the project was to rationally design and prepare single atom alloy (SAA) catalyst compositions based on information gathered from surface science studies on model catalysts and by catalytic evaluation of nanoparticle SAA analogs under realistic conditions. The overarching goal was to use the knowledge garnered from this project to design and develop new catalysts at the single atom limit, which can be applied to selective hydrogenation reactions (alkynes and dienes to alkenes) and the dehydrogenation of methanol and ethanol to value-added products at near-ambient conditions. Detailed information about the results of the project are given below.

Students Involved: George Giannakakis, Sufeng Cao, Mengyao Ouyang, Alex Schilling, Ryan Hannagan

Research Report:

A. Atomically dispersed Pt and Pd on oxides and in alloys for oxidation and dehydrogenation reactions

A.1. An atomic-scale view of single-site Pt catalysts for low-temperature CO oxidation

Supported single atoms are a new class of catalysts in which precious metals can be used at the ultimate efficiency limit. Single atom catalysis begins to merge the fields of homogenous and heterogeneous catalysis, maintaining the tuneability of homogenous catalysts and the ease of product separation and robustness of heterogeneous catalysts. However, despite many recent studies of single atom heterogeneous catalysis, there has been considerable debate regarding the catalytic capabilities of supported single atoms. Furthermore, if single atoms are active, questions remain about their stability, how they bind to the support, and their charge state. Due to the inherent complexity of heterogeneous catalysts, it is difficult to fully characterize the structure and environment surrounding single atoms in a supported catalyst, which are critical for accurate modeling,

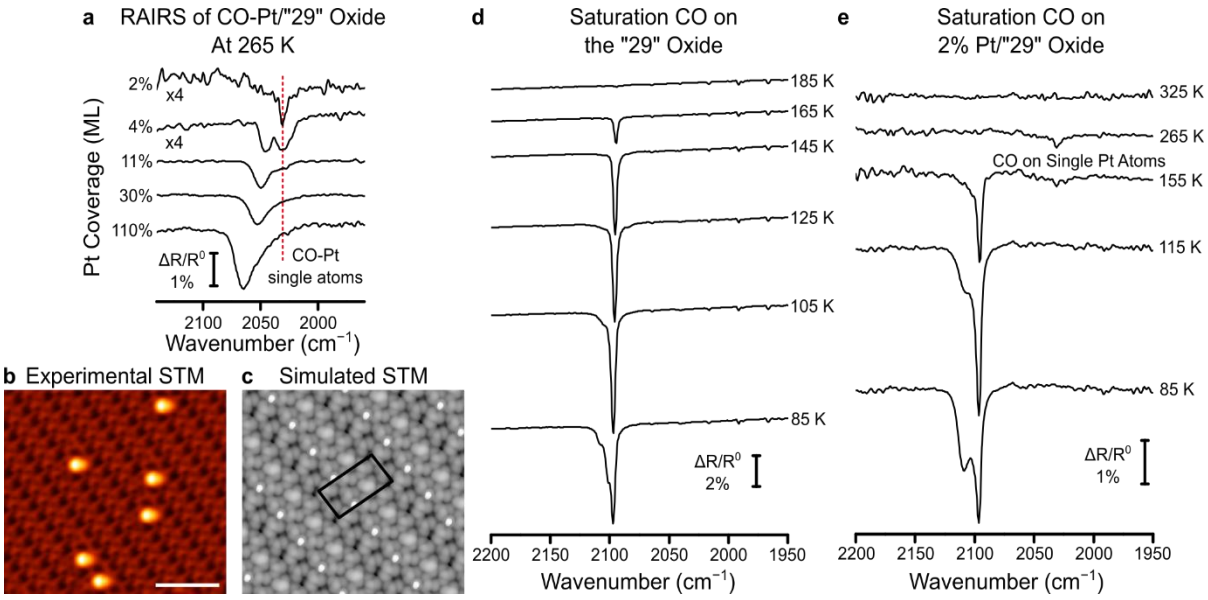

Figure 1. Characterization of CO stretch frequencies at Pt single atoms and nanoparticles. a) RAIRS data of the CO stretch at various Pt coverages at 265 K. **b)** High-resolution STM of 0.5% ML Pt on the "29" copper oxide after adding CO and annealing to 250 K, the scale bar is 5 nm. **c)** Simulated STM image at −0.5 V of the DFT model with a CO-Pt complex in each unit cell, highlighted by the black parallelogram. RAIRS data from an initial CO saturation coverage annealed to various temperatures on **d)** the "29" oxide and **e)** 2% ML Pt on the "29" oxide.[1]

understanding, and the design of new single atom catalysts. For this reason, we use model studies of supported single atoms to investigate the atomic-scale geometric and electronic properties that define their catalytic behavior.

When small amounts of Pt are added to the "29" oxide surface, they remain atomically dispersed, as found by reflection absorption infra-red spectroscopy (RAIRS) and high-resolution STM shown in Fig. 1[1]. The RAIRS data in Fig. 1a show CO stretching bands

for various Pt coverages at 265 K, at which temperature CO has completely desorbed from the oxide support and all the signal is due to CO on Pt sites. These spectra serve as benchmarks for understanding what supported Pt structures give rise to which IR features which is critical to the catalysis community.

Temperature programmed desorption (TPD) was used to study the activity and mechanism of CO oxidation by Pt, shown in Fig. 2. Simultaneously acquired CO_2 and CO TPD traces at various Pt coverages are shown in Figs 2a and b. All CO desorbs molecularly from the "29" oxide below 200 K under the experimental conditions[2], such that in the absence of Pt (0%) no high temperature CO or CO_2 desorption is detected. However, higher temperature desorption is seen when Pt is added to the surface. In both cases of CO_2 and CO desorption, as the Pt coverage is increased above 3% ML, the peak maximum shifts in temperature and a high temperature shoulder forms that is consistent with Pt particle growth[3–6]. Focusing on low Pt coverages in the inset in Figs 2a and b reveals that the CO and CO_2 desorption peaks are first-order in shape and do not shift with change in Pt coverage, indicating that there are negligible lateral interactions due to high dispersion of single Pt atoms in this coverage regime, as found by RAIRS. Shown in Fig. 2a, single Pt atoms yield CO_2 with a peak maximum at 345 K and a CO desorption peak at 350 K. Importantly, CO is more weakly bound to single Pt atoms than to extended Pt surfaces and nanoparticles, which is a promising attribute in terms of resilience toward CO poisoning, which Pt clusters suffer from.

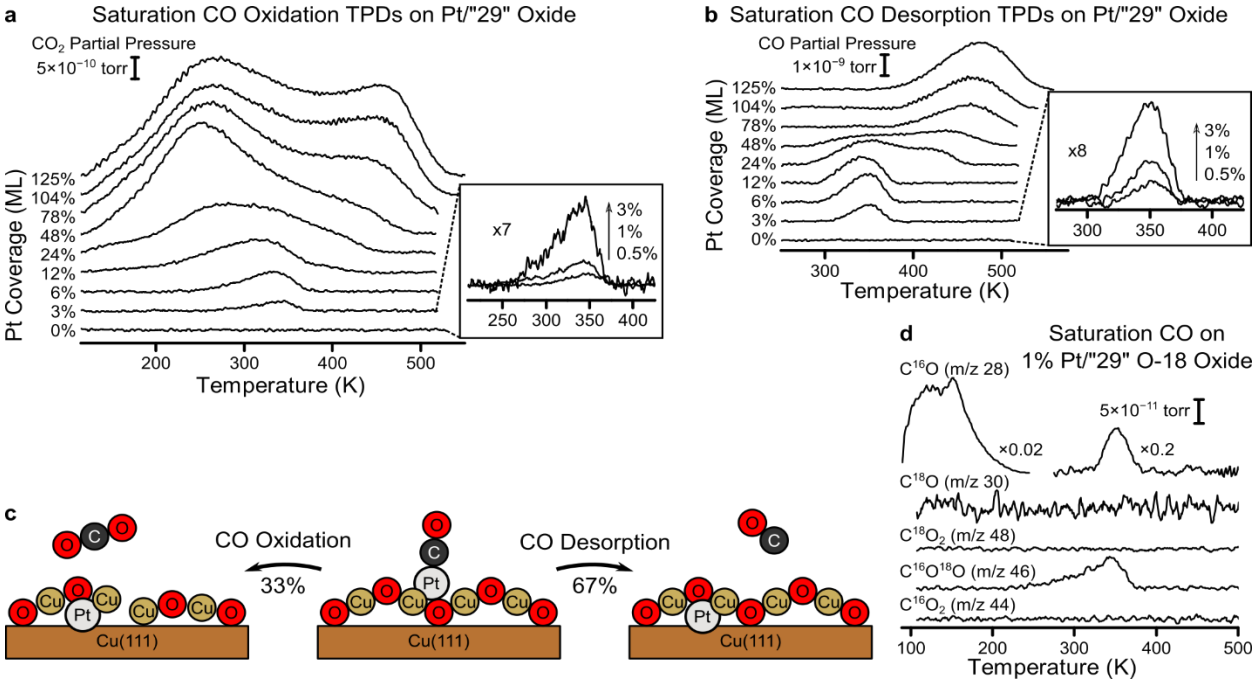

Figure 2. TPD studies of CO oxidation by Pt supported on the "29" copper oxide. a) A family of TPD curves of CO_2 (m/z 44) desorption from saturation CO coverages at different Pt coverages on the "29" oxide. **b)** A family of TPD curves of CO (m/z 28) desorption from the same experiments as in plot a. The insets highlight low Pt coverages at which Pt exists as isolated atoms. **c)** Schematic of the competing pathways for CO oxidation and CO desorption. **d)** TPD after saturation CO exposure on 1% ML Pt supported on an ^{18}O labeled "29" oxide.

X-ray photoelectron spectroscopy (XPS) experiments were carried out to investigate the charge state of single Pt atoms at a coverage of 2% ML during the CO oxidation reaction. Pt grown on metallic Cu(111) was used as a reference for the Pt $4d_{5/2}$ peak. Pt in the absence of CO was first studied. In the case of as-prepared Pt on the "29" oxide support at 150 K, the peak was very broad, consistent with an averaging of Pt species at different binding sites on the surface. XPS identifies the Pt as charge neutral, with the peak centered near the same binding energy as found for Pt(0). The neutral charge of Pt is also consistent with the lower CO stretch frequency found by RAIRS, and agrees with the STS-STM measurements and the DFT model.

A. Water Activation by Single Pt Atoms Supported on a Cu_2O Thin Film

Recent advances in single site catalysis have sparked interest in their use as low-cost and high-efficiency catalysts in a wide variety of reactions. One such reaction that has been heavily studied with single atom catalysts is the water gas shift reaction. In addition, water participates in a rich variety of other industrially important catalytic processes, such as steam reforming reactions.

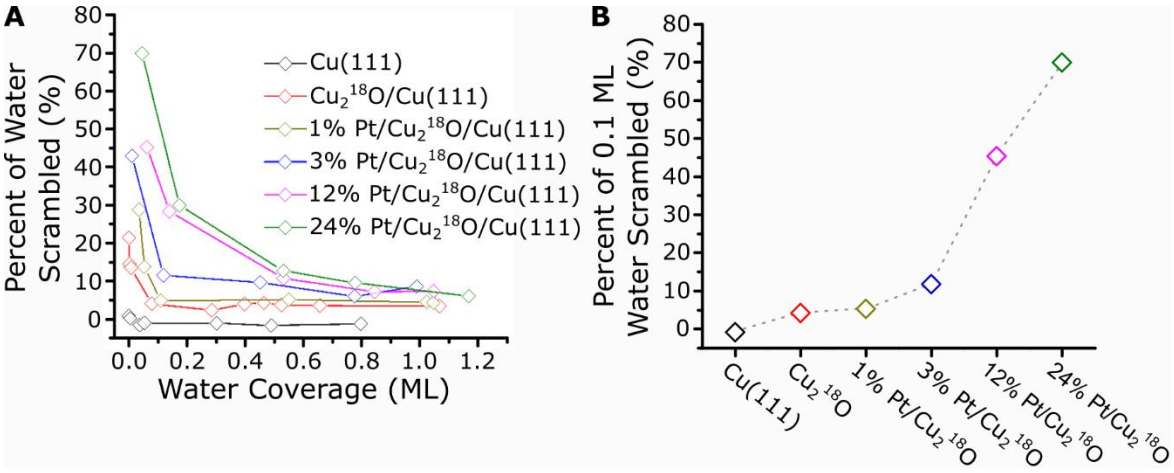

Figure 3. A) The probability of water scrambled for various surfaces as a function of water coverage. B) The probability of water scrambled by the same surfaces at an initial water coverage of 0.1 ML.

Using a model study approach, we found that single Pt atoms supported on the "29" copper oxide film exhibit the ability to activate water as evidenced experimentally via oxygen isotopic scrambling with the support. Coupled with the ability of Pt single atoms to oxidize CO, as we recently reported, these surface science results support and shed light on previous real catalyst findings that highly dispersed Pt atoms on oxide supports are good water-gas shift catalysts. We found that small amounts of isotopic scrambling occur on the bare copper oxide support due to defects, and the degree of scrambling is enhanced in the presence of Pt atoms (Figure 1). This is supported by theory (Jean Sabin McEwen, WSU) in that a much lower energy activation barrier is calculated to exist in the vicinity of Pt atoms as compared to the bare surface oxide support. A viable reaction pathway for water activation and scrambling at single Pt atom sites is proposed. DFT calculations also provide insight into the dynamic relationship between the adsorbate, single Pt atom, and oxide support in order for isotopic scrambling to occur. The results suggest that the Pt-oxide

interface provides a high probability of water dissociation, which facilitates water scrambling, and that this interface is maximized at the single Pt atom limit. As such, this study opens the door to follow up studies on the water gas shift reaction itself and, in particular, how water may assist in the low temperature oxidation of CO.

Surface-Templated Assembly of Molecular Methanol on the Thin Film "29" Cu(111) Surface Oxide

Identifying and characterizing the atomic-scale interaction of methanol with oxidized Cu surfaces is of fundamental relevance to industrial reactions, such as methanol steam reforming and methanol synthesis. In this work, we examined the adsorption of methanol on the well-defined "29" Cu oxide surface using a combination of experimental and theoretical techniques and elucidated the atomic-scale interactions that lead to a unique spatial ordering of methanol on the oxide thin film. We determined that the methanol chain structures form firstly due to epitaxy with the underlying "29" oxide surface. Specifically, the geometry of the "29" oxide is such that there are spatially adjacent $O^{\delta-}$ sites, in the form of O adatoms, and $Cu^{\delta+}$ species, within the Cu_2O-like rings, which allow for methanol to simultaneously bond to the surface via an $O_{methanol}$-$Cu^{\delta+}$ dative bond and an $OH_{methanol}$-$O^{\delta-}$ hydrogen bond. The methanol-oxide bond strength outweighs the strength of the methanol-methanol hydrogen bonds on the "29" Cu oxide, unlike methanol assembly on bare coinage metal surfaces on which hydrogen bonding between adjacent molecules leads to ordered arrays. Secondly, weaker long-range interactions lead to the formation of chains of only *even* numbers of methanol molecules (Figure 2).

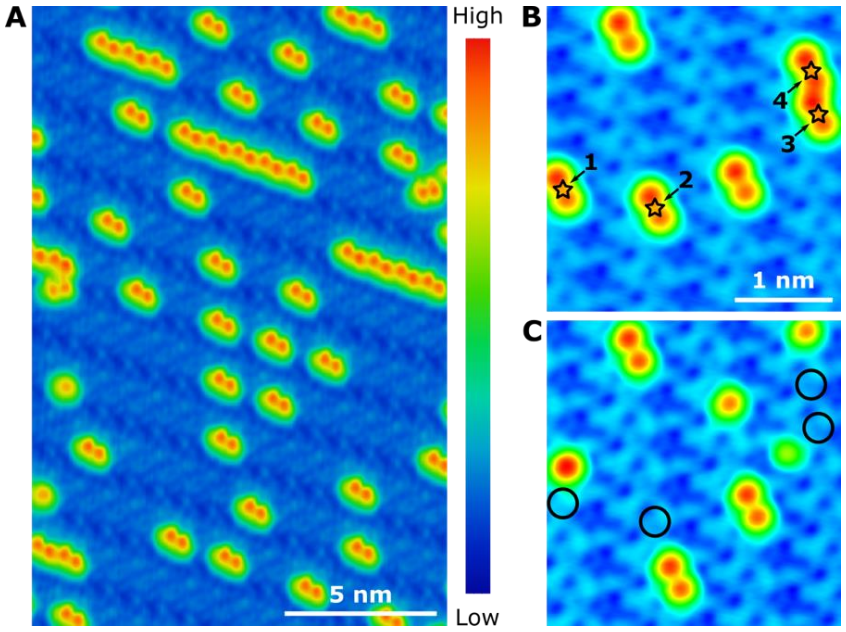

Figure 4. (A) 5 K STM image of methanol molecules on the "29" oxide after a 130 K anneal. Imaging conditions of −0.05 V and 0.05 nA. (B) STM image of the surface before applying 2 V pulses over the points marked with a star. (C) STM image of surface after pulses, in which the circles highlight the pulse location area. Imaging conditions of −0.5

V and 0.05 nA. These experiments reveal that there are no defects beneath the molecules and that the unique self-assembly is substrate rather than molecule-molecule driven.

Overall, the agreement between experimental and theory from TPD, STM, and RAIRS data is evidence toward the accuracy of the proposed "even" dimer structure. It is interesting to note that the molecular chains formed by methanol on the "29" oxide are not due to hydrogen bonding between the adsorbed molecules, as on almost all metal single crystal surfaces. This is analogous to the self-assembly of water on metals being very different from the ice structures formed on oxide surfaces. Instead, methanol adsorption is governed here by the surface-molecule interactions, which comes from a combination of dative bonding with $Cu^{\delta+}$ species and hydrogen bonding with surface $O^{\delta-}$ species. Therefore, unlike the hydrogen bonding driven chains observed on metals, it is actually the structure of the underlying oxide structure that drives the unique even-numbered ordered structures to form. Together, this work reveals that, unlike on metal surfaces, the corrugation of the oxide surface drives methanol adsorption to preferred binding sites, preventing intermolecular hydrogen bonding and dictating the adsorption geometry.

In summary, we have probed many fundamental aspects of single-atom catalysis using a well-defined model system with mono-dispersed Pt atoms in which the atomic-scale geometry and electronic structure of the active sites can be directly probed and correlated to CO oxidation activity. The reaction energetics and a Mars-van Krevelen mechanism, in which lattice oxygen in the close vicinity of the Pt sites is involved in the oxidation process, are confirmed by STM, TPD, and theory. Complementary RAIRS measurements allow the unambiguous assignment of CO stretching frequencies at single Pt atoms, and hence, this work serves as a benchmark for the design and characterization of single atom catalysts. These results also indicate that single supported Pt atoms are capable of performing catalytically relevant reaction steps and that they exist in a neutral charge state, not previously considered to be present at the single atom limit on an oxide support. However, there is a possibility that the underlying metallic copper crystal affects the oxidation state of the Pt atoms. This is currently under investigation by growing thicker copper oxide films that serve to electronically decouple the supported atoms from the underlying metal.

A.2. Activity, Stability, and Selectivity of SAA Pt/Cu (Cu_xO) in CO Oxidation and PROX reactions

Following the tradition that the two groups led by the PI and the co-PI have established[7–13], we are using information from the surface science and theoretical results to inform the synthesis, characterization and testing of Pt/Cu_xO catalytic materials under industrially relevant conditions. This complementary approach informs the design of new catalysts and elucidates their activity/selectivity and stability in a most efficient manner.

In order to investigate Pt/Cu Single Atom Alloys (SAAs) in unsupported form, we prepared nanoporous Cu formats, np-Cu, using the sacrificial support method reported recently for

NiCu single atom alloys[14,15]. Galvanic replacement was subsequently used to deposit isolated Pt atoms in the np-Cu surface, a method that has been used in the past by our group to prepare similar catalytic materials[7,9,12–15]. Lastly, the nanoporous copper particles were oxidized under KOH treatment, which allows for the thermodynamically favorable formation of cuprous oxide (Cu_2O), ultimately forming an oxidized surface layer. BET measurements indicated the formation of a catalyst with moderately high surface area ($10m^2/g$), while the formation of an oxidized surface was verified via XRD (Fig. 3a) to mimic the surface science model with top Cu_2O layer on bulk Cu. TEM imaging provided further proof for a predominant Cu_2O surface, based on the lattice spacing of 0.25nm (Fig. 3c). The atomic dispersion of Pt was verified via CO-DRIFTS, which clearly shows the absence of bridged CO and only yields a peak centered at $2097cm^{-1}$ that is attributed to positively charged Pt[16] (Fig. 3b).

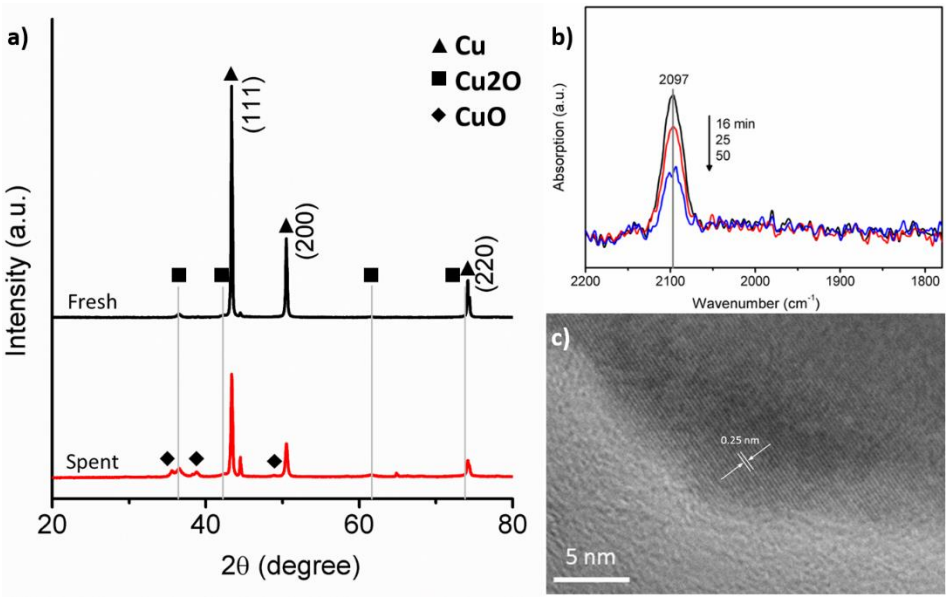

Figure 3. a) XRD measurements for the fresh (upper) and spent after CO oxidation reaction for 15 hours (lower) Pt-np-Cu_xO. **b)** CO DRIFTS of fresh Pt-np-Cu_xO **c)** TEM image of as prepared Pt-np-Cu_xO

The need for efficient Preferential CO Oxidation (PROX) catalysts in industry is well appreciated, especially in the cases of the ammonia synthesis process[17] or the PEM fuel cells technology[18] that requires almost complete elimination of CO from the H_2-rich stream. In both cases, CO acts as a significant catalyst poison and its elimination from the system is therefore essential for the viability of the processes[19]. Having established a remarkable resistance to CO poisoning on Pt atoms in our previous work[13], we decided to employ them as potential dopants of Cu_xO and compared the performance of the bare and the doped support under CO oxidation and CO PROX reaction conditions.

From Figs 4a and 4b it is clear that Pt-np-Cu_xO is more active for CO oxidation regardless of the presence of hydrogen in the feed gas stream. It is also noteworthy that the "light-off" temperature was similar for the two reactions, indicating a similar reaction mechanism. For the Pt doped np-Cu_xO, conversion of CO started at 60°C, while for the bare support at temperatures higher than 90°C. This difference held at 50% and 100% CO conversion as

well. Another important aspect of this catalyst is its excellent selectivity under PROX conditions, which was maintained throughout the temperature range and even at 100% of CO at 170°C (Fig. 4b) for Pt-np-Cu_xO. Even at the highest temperature tested, the conversion of H_2 to H_2O remained below 5%. The absence of CO poisoning[13], along with the negligible coking of the Pt doped materials, as confirmed by TPO, and the mild temperature of operation resulted in a stable catalyst that showed no signs of deactivation, even after prolonged reaction times (Fig. 4c). Based on the above, a new Pt catalyst comprising Pt atoms stabilized in Cu_xO surfaces has been discovered in this work as most promising for CO oxidation and the PROX reaction. This work, still in progress, demonstrates yet another successful bridging of surface science and catalysis.

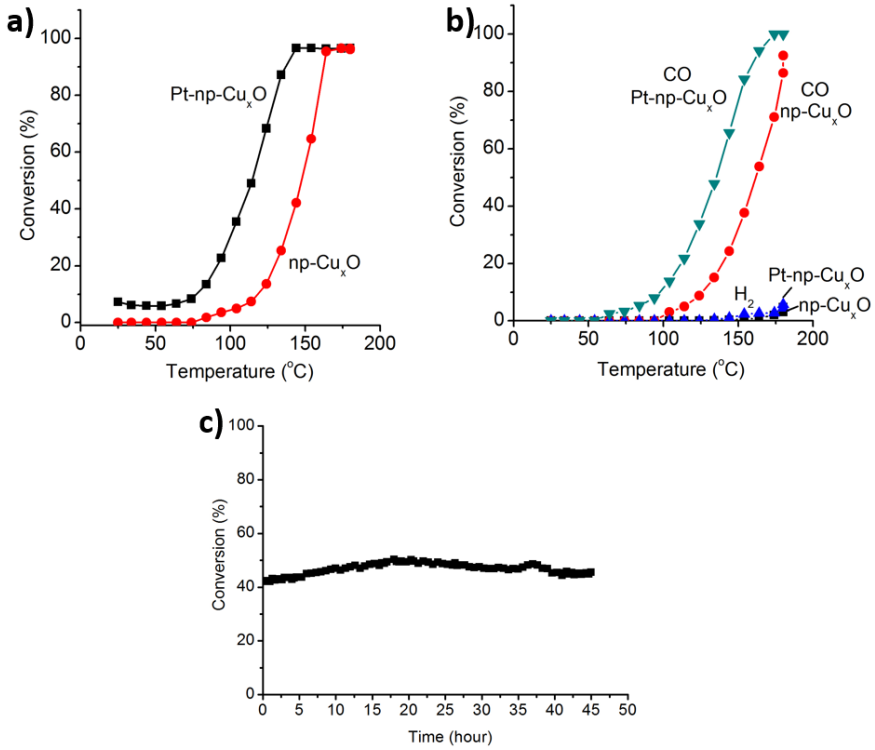

Figure 4. a) Second cycle TPSR data for CO oxidation over Pt-np-Cu_xO and np-Cu_xO, flow rate: 50 mL/min, 2% O_2, 2% CO, bal. He, 500 mg sample **b)** Temperature Programmed PROX oxidation reaction on Pt-np-Cu_xO and np-Cu_xO as control catalyst, flow rate: 50 mL/min, 2% O_2, 2% CO, 40% H_2, bal. He, 500 mg sample **c)** Steady-state PROX at 130°C on Pt-np-Cu_xO, flow rate: 50 mL/min, 2% O_2, 2% CO, 40% H_2, bal. He, 500 mg sample

A.3. Methanol and Ethanol reactivity at Pd/oxide interfaces

In the previous phase of the project, we showed that atomically dispersed gold catalysts supported on $ZnZrO_x$ mixed oxides catalyze the steam reforming of methanol (SRM) and the ethanol dehydrogenation (EDH) reaction with very high selectivity. Single atom gold stabilized by -O bonds (Au-O_x) is the active site, as manifested by the similar TOF values

for atomic gold on all support types. The modification of ZnO with high surface area ZrO_2 efficiently disperses the ZnO phase, providing higher capacity for anchoring and stabilizing the active gold sites. In the current work, we have extended this investigation to Pd. Palladium is cheaper than gold and has better thermal stability than copper-based catalysts. However, Pd catalyzes the alcohol reaction by a different pathway compared to gold and copper-based catalysts. Due to the η^2(C,O)-adsorption of aldehyde species on metallic Pd and PdO, the undesired decomposition of methanol/ethanol takes place on Pd-based catalysts[20], which makes the control of reaction products more complex. Nevertheless, formation of PdZn alloy by high temperature (~400°C) reduction of Pd/ZnO materials modifies the reaction pathway to be similar to that on copper-based catalysts, i.e. no methanol decomposition takes place[20]. Thus, the structure of Pd (PdO, metallic Pd and Pd_xZn_y) influences the reaction pathway in alcohol conversion and lead to different product distribution.

$ZnZrO_x$ material synthesized by the carbon black hard-template method was employed as the catalyst support for palladium[21]. Pd on $ZnZrO_x$ was studied for its potentially better dispersion than on ZnO alone. Fig. 5 shows the comparison between the as prepared and the catalyst after reduction at 400°C for methanol steam reforming and ethanol dehydrogenation reaction. The former shows a mixture of products including CO, while the latter makes exclusively CO_2 and H_2 (SRM) and CO_2/acetaldehyde (EDH). In the case of methanol, detection of the intermediate of methyl formate on reduced Pd/Zn_1Zr_1Ox and Pd/ZnO proved the methanol self-coupling reaction mechanism of SRM on this type catalyst. The same apparent activation energy of SRM on reduced Pd/Zn_1Zr_1Ox and Pd/ZnO further shows that similarly structured active sites are present on both catalysts. Reduction of the catalyst with H_2 at high temperature (400°C) is needed to create the PdZn alloy phase that is active and selective for the SRM reaction. And the formation of PdZn alloy catalyzes exclusively the ethanol dehydrogenation pathway, shutting off the ethanol decomposition reaction. Pd/ZnO reduced at 200°C is not fully converted to alloy, resulting in the formation of CO. Thus, the unique properties of PdZn alloy motivate the mechanistic study of methanol/ethanol reactions on Pd, and is worthwhile to examine for higher carbon alcohols dehydrogenation as well as hydrocarbon dehydrogenation reactions.

To gain a better understanding of the structure of Pd catalysts under different atmospheres, *in situ* XANES/EXAFS was performed for the as prepared (oxidized), H_2 reduced (400°C) and under reactive-atmosphere catalysts. Fig 6. shows that $Pd/Zn_1Zr_1O_x$-P catalyst contains Pd-O and Pd-Pd_{FCC} bonds, typical for the presence of PdO nanoparticles. After H_2 reduction at 400°C, the fitted result of $Pd/Zn_1Zr_1O_x$-R400 corresponds well with crystal structure of β-PdZn alloy and this structure is retained during the reaction. Thus, the unique structure of β-PdZn alloy formed under 400°C H_2 reduction secures the highest H_2 selectivity in SRM; and selective C-H scission, not C-C bond scission, in the EDH reaction. Further mechanistic understanding of the unique PdZn behavior deriving from either site isolation of Pd atoms or specific electronic structure due to the neighboring atoms is still needed.

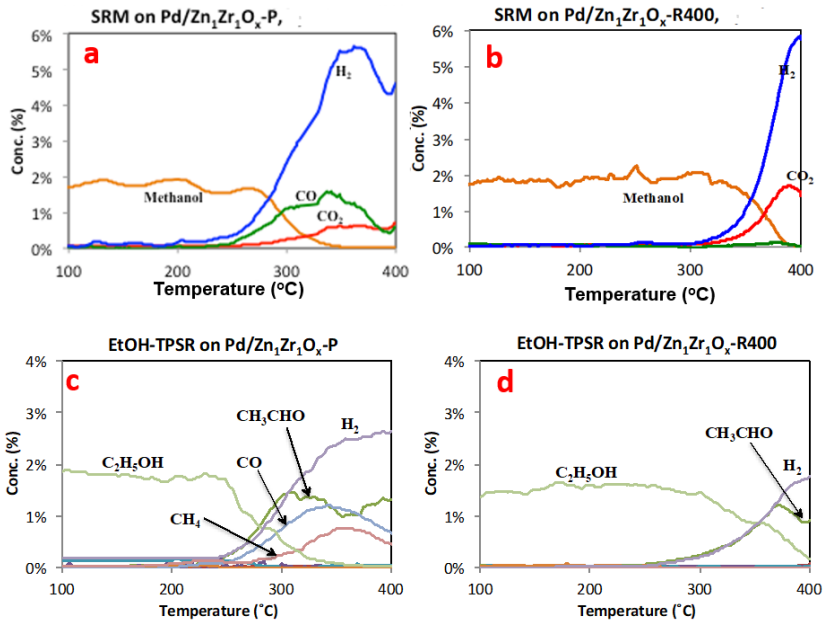

Figure 5. SRM-TPSR on a) as prepared (oxidized) and **b)** H_2-reduced (400°C) 1 wt.% $Pd/Zn_1Zr_1O_x$, flow rate: 25 mL/min, 2% CH_3OH, 2.6% H_2O, bal. He, 100mg sample. **Ethanol/He-TPSR on c)** as prepared (oxidized) and **d)** H_2-reduced (400°C) 1 wt.% $Pd/Zn_1Zr_1O_x$, flow rate: 50 mL/min, 100mg sample

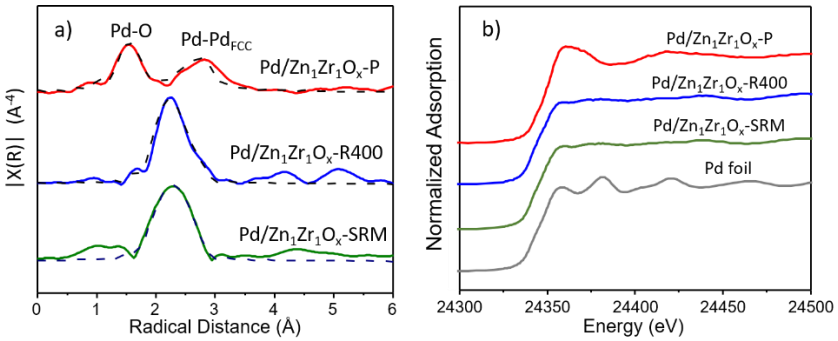

Figure 6. a) Pd K-edge EXAFS magnitude of the Fourier-transform **b)** Normalized XANES data of $Pd/Zn_1Zr_1O_x$-P, $Pd/Zn_1Zr_1O_x$-R400 and $Pd/Zn_1Zr_1O_x$-SRM. The best fitting of the EXAFS spectra is expressed by the dashed line. Traces are offset for clarity.

B. Inorganometallic single site Au/Pt oxo-clusters stabilized by alkali ions as catalysts for the non-oxidative methanol coupling and PROX reactions

B.1. *In situ* CH_3OH IR and DFT study of methanol dehydrogenation over Au_1-Ox-Na_9-$(OH)_y$

A novel and practical method to prepare inorganometallic oxo-clusters of single gold and platinum atoms in alkaline solutions was developed in our lab. For gold, $Au(OH)_3$ was dissolved in NaOH or KOH solutions at ~ 80°C, with 9~10:1 ratio of Na/K to Au. Up to 1.2 wt.% loading of gold was achieved by incipient wetness impregnation of titania with these solutions. This is among the highest loadings of single gold atoms reported to date. EXAFS analyses indicate that Au is coordinated with -O only in the first shell and with Na as the sheath for Au_1-Ox-Na/K_9-$(OH)_y$. Non-oxidative dehydrogenation of methanol

($2CH_3OH \rightarrow HCOOCH_3 + 2H_2$) to methyl formate (coupled product) and hydrogen with 100% selectivity even at high conversions took place over Au_1-Ox-Na_9-$(OH)_y/TiO_2$. Interestingly, and most importantly, the intact complex could be washed out of the support in water, and re-used to impregnate the support without loss of activity. This finding led us to prepare unsupported catalysts, i.e. the same complex after drying, in order to check for the absence of support interaction. Indeed, the unsupported material was active and selective, as shown by our catalytic tests, and by several characterization methods.

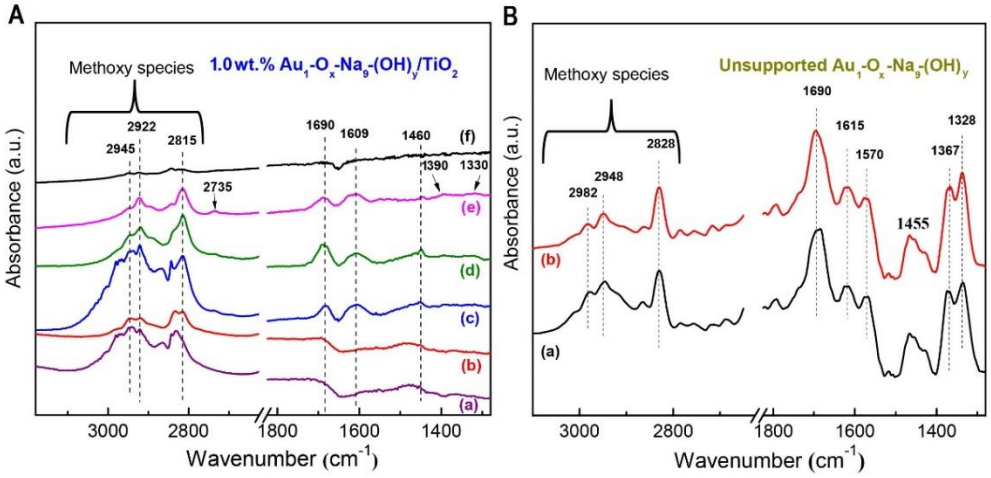

Figure 7. *In situ* CH_3OH DRIFT spectra on supported and unsupported Au_1-O_x-Na_9-$(OH)_y$. (A) 1.0 wt.% Au_1-O_x-Na_9-$(OH)_y/TiO_2$ under: (a) CH_3OH- saturated He flow at RT; (b) pure He at RT after (a); (c) CH_3OH- saturated He flow at 160°C after (b); (d) pure He at RT after (c); (e) 0.5 h in pure He at 160°C and (f) 2 h in pure He at 170°C after (d). **(B)** ODH of methanol on unsupported Au_1-O_x-Na_9-$(OH)_y$ under 1% O_2/He at RT following saturation with CH_3OH at RT after (a) 20 min in He stream and (b) 50 min in He stream.

In situ CH_3OH-DRIFT spectra were collected on both supported and unsupported materials. As shown in Fig.7A(a), the CH_3OH featuring peaks dominate at RT and methoxy species (2945, 2922, 2815 and a broad peak at 1460-1470 cm^{-1}) were observed after sweeping the gas phase CH_3OH by He (Fig. 7A(b)). After switching to reaction conditions, formate (1609, 1390 and 1330 cm^{-1}) and formaldehyde (1460 cm^{-1}) were detected (Fig. 7A(c)). Quenching the sample after reaction conditions, the adsorbed methyl formate (1690 cm^{-1}) was captured (Fig. 7A(d)). Upon ramping the temperature to 160°C under He, the peak of formaldehyde and methyl formate (MF) gradually decreased due to the continuing reaction of formaldehyde and methoxy and the desorption of MF product; but the intensity of the formate peak, identified as spectator species, remained unchanged (Fig. 7A(e)). Further increasing the temperature to 170°C for 2h, all adsorbed species disappeared due to desorption. The production of MF was also detected on unsupported Au_1-O_x-Na_9-$(OH)_y$ with assisting of O_2 at RT (Fig. 7B), which demonstrates that the single atom [Au-O_x]- is the catalytic site for methanol dehydrogenation and methanol coupling reaction to produce the ester and hydrogen[19].

The experimental results (capturing catalytic sites, and intermediate/spectator species) were complemented by theoretical studies aimed at gaining further mechanistic insight into the catalytic activity of the [Au_1-O_x]- species toward MF production. To this end, our

collaborators at Wisconsin performed a detailed study of the thermochemistry of relevant steps, using density functional theory (DFT), to efficiently screen cluster model candidates, starting from the analogous clusters we studied in previous work[17]. On these clusters, it was discovered that methanol dehydrogenation proceeds downhill to form dioxy methylene instead of formaldehyde. The dioxy methylene species dehydrogenation to formate (HCOO) is highly exothermic, thus resulting in the HCOO spectator which was detected by the *in situ* DRIFTS study. Recognizing the need for any active site model to retain cationic nature of the Au center in the presence of formate spectator species, we designed the active site models with DFT, subject to the following constraints: i) the active site must retain a Bader charge on Au of approximately +0.41 eV to resemble the working Au(I) catalyst, and ii) upon initiation of the catalytic cycle, the favored product of methanol/methoxy dehydrogenation must be formaldehyde, as opposed to dioxy-methylene species (the precursor of HCOO). Accordingly, three new cluster models evolved from previously examined spectator-free models: Au_1-O_3-Na_9-$(OH)_9$, Au_1-O_7-Na_9-$(OH)_5$, and Au_1-O_9-Na_9-(OH) with the last two being permanently decorated with two HCOO groups, while the first is decorated with a single HCOO group.

The computational minimum energy path for Au_1-O_3-Na_9-$(OH)_9$ is presented in Fig. 8. The cluster was decorated by spectator species HCOO, in agreement with the IR findings (Fig. 7). Adsorption of a second methanol prior to the desorption process is proposed here. In this path, an additional methanol will adsorb exothermically (-0.68 eV) prior to the coupling reaction to MF. A two-step desorption process is followed, in which (MF + 3/2 H_2) are desorbed with a slight barrier of 0.40 eV, followed by the desorption of 1/2 H_2 (0.83 eV) after further dehydrogenation of the remaining methoxy to formaldehyde. The desorption of 1/2 H_2 is shown by a thick red arrow in Fig. 8, and represents the most difficult step in the reaction network. Its thermodynamic barrier (~80 kJ/mol) is in good agreement with the experimentally measured apparent activation energy barrier (~95 kJ/mol). The H abstraction is much easier from H_2O-like intermediates than from -OH. The structure of this gold oxo cluster evolved (became more open) under reaction conditions, with the Au atom less coordinated with -O, and thus being prone to binding the formaldehyde intermediate.

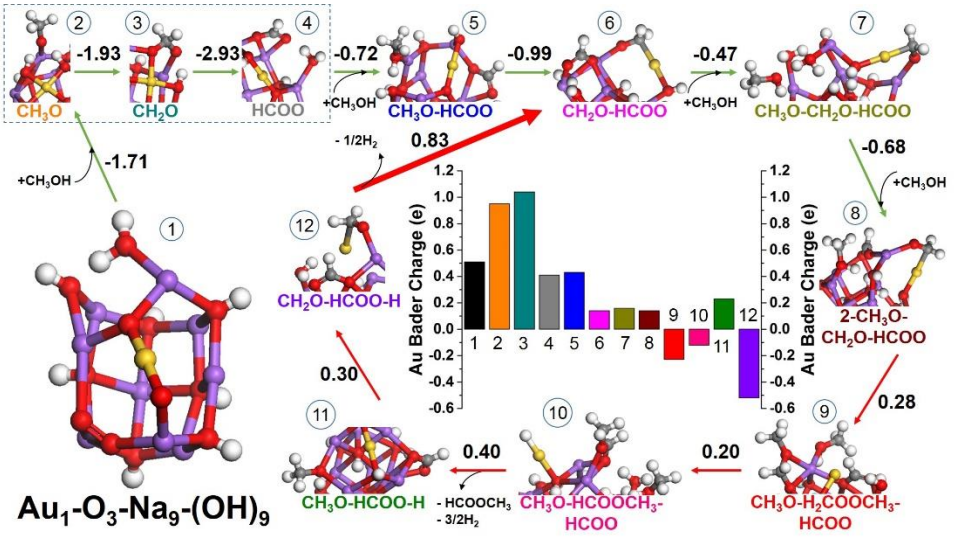

Figure 8. AIMD-calculated minimum energy structures and their energetics along the minimum energy pathway from methanol to MF + 2 H_2 on Au_1-O_3-Na_9-$(OH)_9$, starting from the undecorated cluster, followed by the formation of 1-HCOO spectator on the cluster to form the working active site, and then the catalytic cycle. Au, Na. C, O, and H atoms are represented by yellow, purple, grey, red, and white spheres, respectively[22].

B.2. Single Pt atom catalysts stabilized by -O-Na/K as highly active and selective water-gas-shift (WGS) and preferential CO oxidation (PROX) catalysts

Alkaline ions were found effective to stabilize precious metal atoms (Pt, Au), thus increasing the number of the single metal atom active sites on any support significantly[23–27]. A new protocol is introduced here for platinum, whereby insoluble $H_2Pt(OH)_6$ reacts with alkaline solution to obtain transparent Pt complex solution, and single Pt atom site catalysts can be made by incipient wetness impregnation of the solution onto any support.

EXAFS results of supported Pt_1-O_x-Na_9-$(OH)_y/Al_2O_3$ indicate that Pt is coordinated with -O and no Pt nanoparticles were formed (Fig. 9A). The supported Pt_1-O_x-Na_9-$(OH)_y/Al_2O_3$ catalyst has more Pt atoms anchored by -O and OH groups and hence is more active for WGS compared to Pt/Al_2O_3 (Fig. 9B).

As discussed above, the PROX reaction is an attractive option to purify H_2 by selectively removing CO by CO oxidation, significantly reducing the loss of energy and H_2. A good catalyst should have: 1) a high loading of the Pt atom active sites; 2) high activity for CO oxidation; 3) negligible activity for H_2 oxidation over a wide temperature window. Single Pt atom catalysts are reported as efficient towards CO oxidation because they adsorb CO weakly[16,28]. Moreover, the cationic Pt atom is expected to have poor H_2 dissociation activity; hence low ability to catalyze H_2 oxidation[21]. Accordingly, our single Pt atom stabilized by alkaline ions (K) catalysts are expected to have superior activity for CO oxidation and very high O_2 selectivity. This is precisely what we found (Fig. 9C).

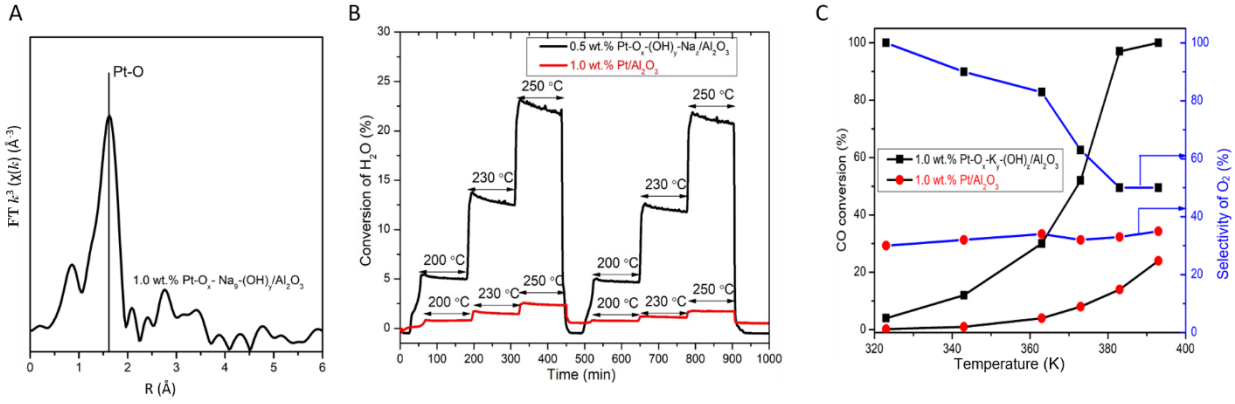

Figure 9. (A) Fourier transformed (FT) k^3-weighted $\chi(k)$-function of the EXAFS spectra of 0.5 wt.% Pt-O_x-$(OH)_y$-Na_z/Al_2O_3, R(Å), distance in Angstroms;
(B) WGS tests over Pt_1-O_x-$(OH)_y$-Na_z/Al_2O_3 and Pt/Al_2O_3, 1.0 wt% Pt/Al_2O_3 was prepared by incipient wetness impregnation (IWI) of $Pt(NH_3)_4(NO_3)_2$ onto γ-Al_2O_3 and 0.5 wt.% Pt-O_x-$(OH)_y$-Na_z/Al_2O_3 made by impregnating the alkaline solution of the platinum complex onto γ-Al_2O_3, flow rate: 30 mL/min 10 vol.% CO, 3 vol.% H_2O, 100mg sample

(C) PROX tests on Pt_1-O_x-$(OH)_y$-Na_z/Al_2O_3 and Pt/Al_2O_3, flow rate: 42 mL/min, 1 vol.% CO, 1 vol.% O_2, 40 vol.% H_2, bal. He, 100mg sample

C. Single-atom alloys

C.1. PtCu single-atom alloy catalysts for coke resistant C-H activation and selective dehydrogenation of n-butane

The production of shale gas from hydraulic fracturing has boosted the supply of light alkanes such as ethane and propane in recent years[29,30]. We focused on the dehydrogenation of alkanes to produce alkenes, which are precursors to industrially relevant polymers[29,31–33]. Preventing coking is indeed an active, yet challenging area of current research[34]. Here, we demonstrate that PtCu SAAs activate C-H bonds with significantly improved activity over Cu, while avoiding coking that occurs on catalysts with extended Pt ensembles due to the ability of Cu to facilitate C-C coupling chemistry.

$Pt_{0.03}$Cu-SAA and $Pt_{0.01}$Cu-SAA nanoparticles (NPs) were prepared by a galvanic replacement reaction as reported in Lucci et al. and Liu et al.[8,13] and were supported on silica. We conducted EXAFS and FTIR studies to confirm the formation of Cu NPs with embedded isolated Pt atoms[12].

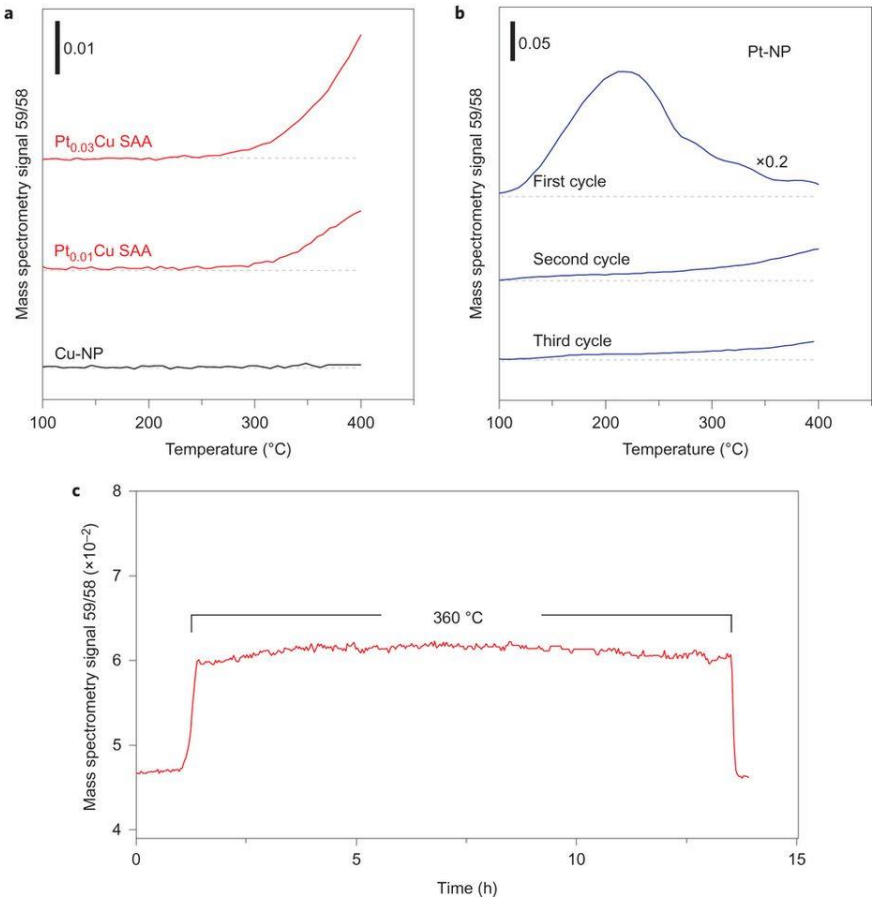

Figure 10. TPSR data for the B-D scrambling reaction over (a) $Pt_{0.03}$Cu-SAA, $Pt_{0.01}$Cu-SAA and Cu-NP catalysts and (b) Pt-NP catalysts, monitored by mass spectrometry. (Temperature ramp 5°C/min) The data in (a) are from the second reaction cycle. First, second and third cycles of TPSR are shown for Pt-NP (b); (c) 12-hour test for the $Pt_{0.01}$Cu-SAA catalyst at 360°C showing stability over time. The catalyst was at room temperature at the beginning and end of the test, flow rate: 50 mL/min, 5% butane, 2% deuterium, bal. Ar, 100 mg sample[12]

Butane – deuterium scrambling (B-D scrambling)

We compared the performance of Cu NPs and PtCu SAA NP catalysts for B-D scrambling using temperature programmed surface reaction (TPSR) (Fig. 10). The production rate of deuterated butane in B-D scrambling experiments indicates the C-H activation capability of the catalysts[8,13]. The second cycle data are plotted here as there is no activity difference between the second and third cycle. In Fig. 10, the ratio between mass 59 and 58 reflects the ratio between deuterated butane (C_4H_9D) and butane (C_4H_{10}). $Pt_{0.03}$Cu-SAA and $Pt_{0.01}$Cu-SAA start to convert butane (C_4H_{10}) to deuterated butane (C_4H_9D) at around 250 °C but Cu-NP is active only at temperatures above 500 °C. This demonstrates that the activity of B-D scrambling i.e. C-H activation, is significantly improved by the addition of a small amount of isolated Pt atoms into the Cu surface. At the same condition, the silica support is not active for B-D scrambling.

Monometallic Pt NP catalysts rapidly deactivate during the reaction (Fig. 10b). In the first cycle of TPSR, the production of C_4H_9D 'lights-off' at 100 °C and increases with increasing temperature up to 230 °C. The production rate of C_4H_9D then drops off after 230 °C indicating significant deactivation, overcoming the effect of temperature increase on reaction rate. The second and third cycles of TPSR show much lower activity compared to the first cycle and the activity decreases cycle by cycle. On the other hand, PtCu-SAAs are very stable. Fig. 10c shows that $Pt_{0.01}$Cu-SAA catalyzes the B-D scrambling at 360 °C without any deactivation for at least 12 hours.

We performed temperature-programmed-oxidation (TPO) of used catalysts to determine whether carbon deposition occurs during B-D scrambling. Pt-NPs and $Pt_{0.01}$Cu-SAAs were both exposed to B-D scrambling conditions at 360 °C for 12 hours prior to TPO measurements. A broad CO_2 evolution from the used Pt-NP is seen, beginning at 130 °C. These features are absent on the $Pt_{0.01}$Cu-SAA. Thus, PtCu SAAs are coke-resistant at the reaction conditions used here, while Pt NPs catalyze carbon formation and deposition, which causes severe deactivation of the catalyst during the B-D scrambling conditions.

Nonoxidative dehydrogenation of butane

Encouraged by the success in the coke resistance B-D scrambling with SAA catalysts, we explored the nonoxidative dehydrogenation of butane with SAA catalysts. At 400 °C, $Pt_{0.01}$Cu-SAA stably converts butane to butene for at least 52 hours without any deactivation. An Arrhenius- type plot for butane dehydrogenation over $Pt_{0.01}$Cu-SAA and Pt-NP catalysts is shown in Fig. 11. The apparent activation energy of the reaction over $Pt_{0.01}$Cu-SAA and Pt-NP is 112 and 51 kJ/mol, respectively. The rate limiting step for light alkane dehydrogenation is likely the first C-H bond activation. We have found the C-H activation barrier over $Pt_{0.01}$Cu-SAA is higher than that of Pt-NP from the B-D scrambling tests[12]. Thus, the trend we observed in the apparent activation energy of butane

dehydrogenation is in agreement with the trend in the C-H activation barrier. The high stability of $Pt_{0.01}Cu$-SAA in butane dehydrogenation conditions is also in agreement with its stability in B-D scrambling conditions. Therefore, we have demonstrated the SAA Pt/Cu alloy as a most promising catalyst for alkane dehydrogenation. Work is continuing to rank order other M/Cu SAAs (M: Pt, Pd, Rh, Ni, …) and improve our mechanistic understanding of these systems.

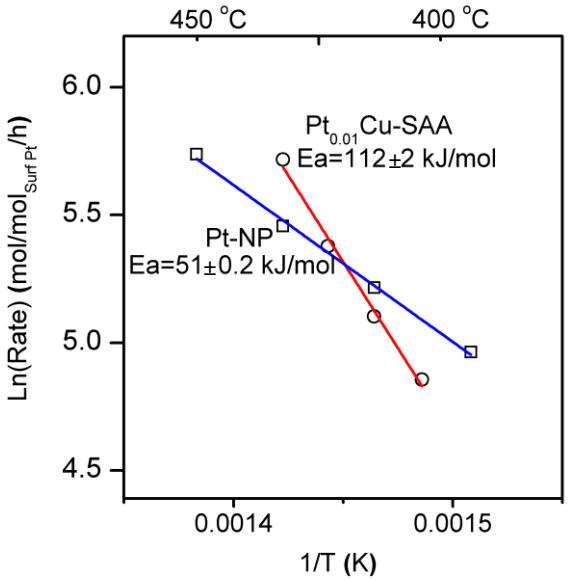

Figure 11. Arrhenius-type plot. The reaction rate of butane dehydrogenation was measured between 450 and 390 °C with conversion below 10%, flow rate: 50 mL/min, 2.5% butane, 5% H_2, bal. He, 30-80 mg sample[12].

C.2. NiAu Single Atom Alloys as Model and Realistic Catalysts for Selective Hydrogenation Reactions

Silica-supported NiAu alloys were prepared in nanoparticle form (NPs) following a sequential reduction method[35] First, PVP-Au colloids were synthesized as described by Tedsree et al.[36] by adding the gold precursor ($HAuCl_4$) in a solution of ethylene glycol and PVP in N_2 gas atmosphere. Formation of Au NPs was then achieved by addition of $NaHCO_3$ and heating at 90 °C. After cooling at room temperature, the appropriate amount of nickel precursor ($NiCl_2$) was added into the solution along with small amounts of hydrazine and NaOH solution. After pre-activation and purging of organic impurities by heating at 650 °C, silica was suspended in ethanol and the catalyst-containing solution was added dropwise under sonication. The supported NPs were extracted by filtration, washing, drying and calcination at 400 °C. The gold metal loading on the support was measured to be 5% in all samples, based on inductively coupled plasma (ICP) elemental analysis.

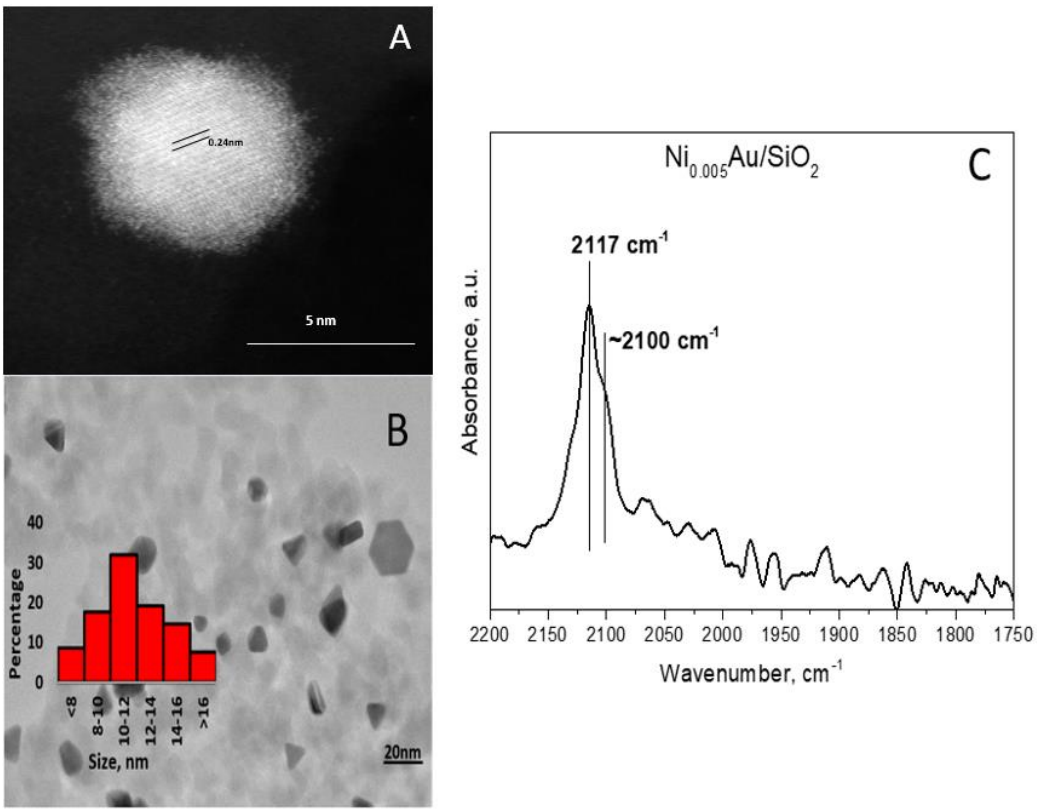

Figure 12. STEM image and lattice spacing (A) TEM image and size distribution of nanoparticles (B) and CO DRIFT spectrum (C) of $Ni_{0.005}Au/SiO_2$

Characterization of NiAu NPs with TEM verified the absence of Ni planes (formation of Ni clusters) as the lattice spacing which was equal to 0.24 nm (Fig. 12 A) is in good agreement with the [111] lattice planes of Au[37]. An average particle size of 12 nm size was calculated from the TEM images, Fig. 12B. CO DRIFT spectra for NiAu NPs were recorded like the one shown in Fig. 12 C. CO adsorption on the surface of $Ni_{0.005}Au/SiO_2$ shows characteristic peaks of atop Au^0-CO monocarbonyl modes by a peak at 2117 cm^{-1} along with sub-carbonyl species $Ni^0(CO)_x$ with x=2 or 3 which were detected by a shoulder around 2100 cm^{-1} [38,39]. The absence of peaks in the 2050-2060 cm^{-1} region, which have been attributed to CO adsorbed on Ni clusters[40], is indicative of the lack of the latter and thus provides strong evidence for the atomic dispersion of Ni on Au NPs. As reported in our previous work, H atoms do not spillover from Pd atoms to Au under UHV studies[41,42]. In the same way, we expect that in NiAu SAAs presented here, isolated Ni atoms will provide a limited amount of H atoms per active site. For selective hydrogenations of α,β-unsaturated aldehydes where the goal is to selectively hydrogenate the C=O and not the C=C bond, NiAu SAAs are a promising material. Hydrogenation reactions of acrolein and methacrolein over these materials will be tested in batch and semi-batch reactor systems. In addition, in-situ monitoring of the solid catalyst/liquid interface will take place in a flow reactor system combining an attenuated total reflection system infrared spectroscopy (ATR-IR) cell with an HPLC system for analysis of liquid products reaction mixture. These new reactions/reactor systems will be the subject of our future study in the project.

Accelerated Cu_2O Reduction by Single Pt Atoms at the Metal-Oxide Interface

The reducibility of metal oxides, when serving as the catalyst support or the active sites themselves, plays an important role in heterogeneous catalytic reactions. For example, in the production of methanol from CO_2 hydrogenation with Cu-based catalysts, the degree of surface oxidation plays a critical role in catalyst performance. We performed a combination of experimental and theoretical studies that demonstrate how the addition of small amounts of atomically dispersed Pt at the metal/oxide interface dramatically enhances the reducibility of a Cu_2O thin film by H_2. X-ray photoelectron spectroscopy (XPS) and temperature-programmed desorption (TPD) results reveal that upon oxidation, a PtCu single-atom alloy (SAA) surface is covered by a thin Cu_2O film and, therefore, it is unable to dissociate H_2. Despite this, *in situ* studies using ambient pressure (AP) XPS (**Figure 1**) showed that the presence of a small amount of Pt under the oxide layer can, at the single-atom limit, promote the reduction of Cu_2O by H_2 at room temperature. Density functional theory calculations indicate that the increased activity is due to the presence of atomically dispersed Pt under the oxide layer, which weakens the Cu-O bonds in its immediate vicinity, thus making the interface between subsurface Pt and Cu_2O a nucleation site for the formation of metallic Cu. This first step in the reduction process results in the presence of surface Pt atoms surrounded by metallic Cu patches, and the Pt atoms become active for H_2 dissociation, which consequently accelerates the reduction of the oxide layer.

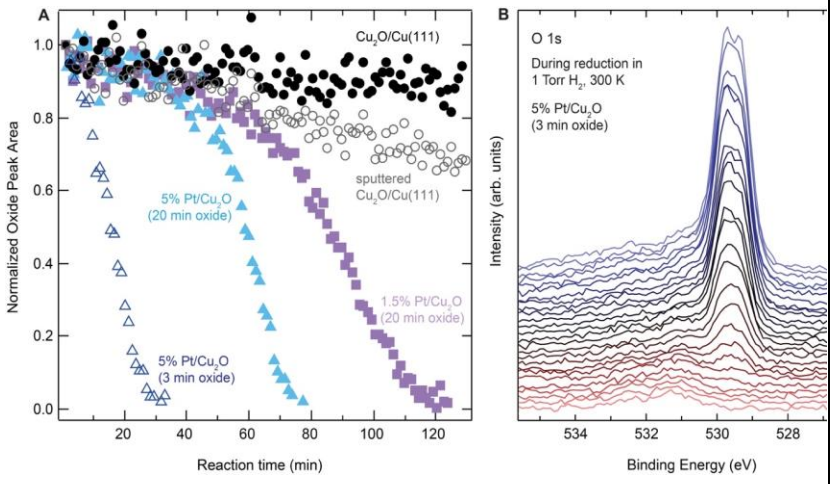

Figure 1: In situ monitoring of effect of Pt on the reduction of a Cu_2O film. (A) Plot of normalized oxide peak area as a function of reaction time in 1 Torr of H_2 at 300 K for bare Cu_2O/Cu(111) (closed circles), lightly sputtered Cu_2O/Cu(111) (open circles), 1.5% Pt/Cu_2O(20min) (squares), 5% Pt/Cu_2O(20min) (closed triangles), and 5% Pt/Cu_2O(3min) (open triangles). (B) O 1*s* AP-XPS spectra during the reduction of 5% Pt/Cu_2O(3min) in 1 Torr of H_2 at 300 K acquired every 70 seconds.

This finding has important implications in catalysis science since the seemingly inert oxide-covered Pt/Cu SAA is actually able to promote the reduction of the oxide due to the presence of dopant single Pt atoms under the oxide, thus creating nucleation sites for the formation of metallic Cu. These insights into the reactivity of metal/oxide interface sites toward H_2 activation and their effect on the subsequent reduction of the oxide can be used in rational catalyst design efforts for reactions where interface regions are key to high activity and prone to deactivation. For Cu-based methanol synthesis catalysts, for example, the addition of a small amount of Pt dopant, at the single atom

limit, could provide a way to maintain a reduced state of Cu under relatively mild reaction conditions where H_2 dissociation may be rate limiting and these ideas are currently being tested for nanoparticle and nonporous PtCu catalysts.

High-loading Single Pt atom sites [Pt-O(OH)x] catalyze the CO PROX reaction with high activity and selectivity at mild conditions

Hydrogen is an important chemical used in ammonia synthesis, methanol synthesis, hydrogenation reactions, and in clean power generation by fuel cells. The preferential oxidation of CO (PROX) in hydrogen-rich fuel gas streams is an attractive option to purify H_2, which significantly reduces the loss of energy and H_2. It is challenging to achieve high CO conversion with concomitant high selectivity to CO_2 but not H_2O. We report the synthesis of high-loading single Pt atom (2.0 wt.%) catalysts with oxygen bonded alkaline ions that stabilize the cationic Pt (**Figure 2**). The synthesis occurs in aqueous solution and achieves high Pt atom loadings in a single-step incipient wetness impregnation of alumina or silica. Surprisingly, these catalysts have high CO PROX selectivity even at high CO conversion (~99.8% conversion; 70% selectivity, 110 ^oC) and good stability under reaction conditions. Importantly, the catalyst activity and selectivity does not depend on the choice on the support. Their impressive catalytic performance originates from a large amount of accessible [Pt_1-O_x] active sites (100 % atom utilization), of low chemical valence during reaction, that remain positively charged during long stability tests. The single Pt atom in our catalysts can activate H_2 and O_2 to generate -OH, which boosts CO oxidation via the water-gas-shift reaction pathway. This work paves the way to synthesize stable, high-loading single-atom catalysts via the alkali stabilizer strategy. These new catalysts are promising candidates for achieving high CO conversion and O_2 selectivity for the CO-PROX reaction which is an increasingly attractive and energy efficient technology.

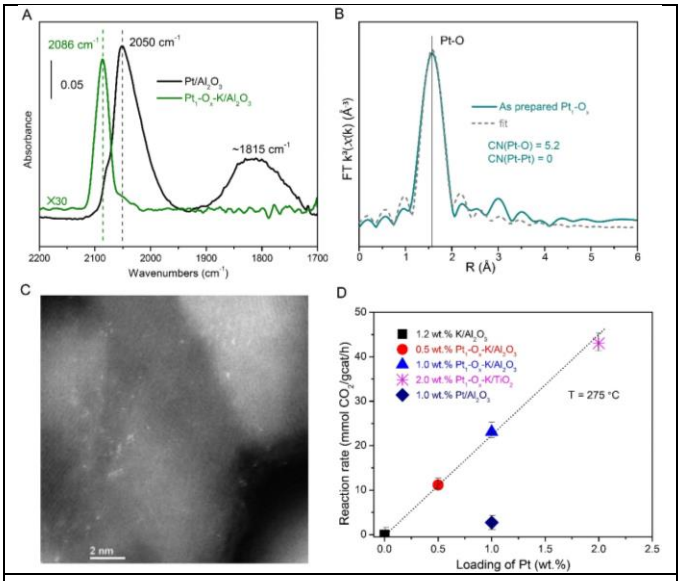

Figure 2. Characterization of as prepared supported Pt catalysts: A. CO DRIFTS of Pt/Al_2O_3 and Pt_1-O_x-K/Al_2O_3; B. EXAFS fitting of as-prepared Pt_1-O_x-K/Al_2O_3; C. Representative ac-HAADF-STEM image of Pt_1-O_x-K/Al_2O_3; D. Plot of WGS activity at 275 °C vs Pt loading of different Pt-based catalysts (30 mL/min, 10 % CO, 3 % H_2O, 100 mg catalyst loading, each data point was obtained by averaging 4 data points of stability test).

References

(1) Therrien, A. J.; Hensley, A. J. R.; Marcinkowski, M. D.; Zhang, R.; Lucci, F. R.; Coughlin, B.; Schilling, A. C.; McEwen, J.-S.; Sykes, E. C. H. An Atomic-Scale View of Single-Site Pt Catalysis for Low-Temperature CO Oxidation. *Nat. Catal.* **2018**, *1*, 192–198.

(2) Hensley, A. J. R.; Therrien, A. J.; Zhang, R.; Marcinkowski, M. D.; Lucci, F. R.; Sykes, E. C. H.; McEwen, J. S. CO Adsorption on the "29" CuxO/Cu(111) Surface: An Integrated DFT, STM, and TPD Study. *J. Phys. Chem. C* **2016**, *120*, 25387–25394.

(3) Gerrard, A. L.; Weaver, J. F. Kinetics of CO Oxidation on High-Concentration Phases of Atomic Oxygen on Pt(111). *J. Chem. Phys.* **2005**, *123*.

(4) Heiz, U.; Sanchez, A.; Abbet, S.; Schneider, W. D. Catalytic Oxidation of Carbon Monoxide on Monodispersed Platinum Clusters: Each Atom Counts. *J. Am. Chem. Soc.* **1999**, *121*, 3214–3217.

(5) Xu, J.; Yates, J. T. Catalytic Oxidation of CO on Pt(335): A Study of the Active Site. *J. Chem. Phys.* **1993**, *99*, 725–732.

(6) Campbell, C. T.; Ertl, G.; Kuipers, H.; Segner, J. A Molecular Beam Investigation of the Interactions of CO with a Pt(111) Surface. *Surf. Sci.* **1981**, *107*, 207–219.

(7) Boucher, M. B.; Zugic, B.; Cladaras, G.; Kammert, J.; Marcinkowski, M. D.; Lawton, T. J.; Sykes, E. C. H.; Flytzani-Stephanopoulos, M. Single Atom Alloy Surface Analogs in Pd0.18Cu15 Nanoparticles for Selective Hydrogenation Reactions. *Phys. Chem. Chem. Phys.* **2013**, *15*, 12187.

(8) Lucci, F. R.; Liu, J.; Marcinkowski, M. D.; Yang, M.; Allard, L. F.; Flytzani-Stephanopoulos, M.; Sykes, E. C. H. Selective Hydrogenation of 1,3-Butadiene on Platinum–copper Alloys at the Single-Atom Limit. *Nat. Commun.* **2015**, *6*.

(9) Shan, J.; Lucci, F. R.; Liu, J.; El-Soda, M.; Marcinkowski, M. D.; Allard, L. F.; Sykes, E. C. H.; Flytzani-Stephanopoulos, M. Water Co-Catalyzed Selective Dehydrogenation of Methanol to Formaldehyde and Hydrogen. *Surf. Sci.* **2016**, *650*, 121–129.

(10) Liu, J.; Shan, J.; Lucci, F. R.; Cao, S.; Sykes, E. C. H.; Flytzani-Stephanopoulos, M. Palladium–gold Single Atom Alloy Catalysts for Liquid Phase Selective Hydrogenation of 1-Hexyne. *Catal. Sci. Technol.* **2017**, *7*, 4276–4284.

(11) Marcinkowski, M. D.; Liu, J.; Murphy, C. J.; Liriano, M. L.; Wasio, N. A.; Lucci, F. R.; Flytzani-Stephanopoulos, M.; Sykes, E. C. H. Selective Formic Acid Dehydrogenation on Pt-Cu Single-Atom Alloys. *ACS Catal.* **2017**, *7*, 413–420.

(12) Marcinkowski, M. D.; Darby, M. T.; Liu, J.; Wimble, J. M.; Lucci, F. R.; Lee, S.; Michaelides, A.; Flytzani-Stephanopoulos, M.; Stamatakis, M.; Sykes, E. C. H. Pt/Cu Single-Atom Alloys as Coke-Resistant Catalysts for Efficient C-H Activation. *Nat. Chem.* **2018**, *10*, 325–332.

(13) Liu, J.; Lucci, F. R.; Yang, M.; Lee, S.; Marcinkowski, M. D.; Therrien, A. J.; Williams, C. T.; Sykes, E. C. H.; Flytzani-Stephanopoulos, M. Tackling CO Poisoning with Single-Atom Alloy Catalysts. *J. Am. Chem. Soc.* **2016**, *138*, 6396–6399.

(14) Shan, J.; Janvelyan, N.; Li, H.; Liu, J.; Egle, T. M.; Ye, J.; Biener, M. M.; Biener, J.; Friend, C. M.; Flytzani-Stephanopoulos, M. Selective Non-Oxidative Dehydrogenation of Ethanol to Acetaldehyde and Hydrogen on Highly Dilute

NiCu Alloys. *Appl. Catal. B Environ.* **2017**, *205*, 541–550.
(15) Shan, J.; Liu, J.; Li, M.; Lustig, S.; Lee, S.; Flytzani-Stephanopoulos, M. NiCu Single Atom Alloys Catalyze the C-H Bond Activation in the Selective Non-Oxidative Ethanol Dehydrogenation Reaction. *Appl. Catal. B Environ.* **2017**, *226*, 534–543.
(16) Jones, J.; Xiong, H.; DeLaRiva, A. T.; Peterson, E. J.; Pham, H.; Challa, S. R.; Qi, G.; Oh, S.; Wiebenga, M. H.; Hernández, X. I. P.; *et al.* Thermally Stable Single-Atom Platinum-on-Ceria Catalysts via Atom Trapping. *Science.* **2016**, *353*, 150–154.
(17) Schlögl, R. Inorganic Reactions - Ammonia Synthesis. In *Handbook of Heterogeneous Catalysis*; Ertl, G.; Knozinger, H.; Schuth, F.; Weikamp, J., Eds.; Wiley-VCH Verlag GmbH & Co. KGaA: Weinheim, Germany, 2008; Vol. 4–5, pp. 2501–2575.
(18) Baschuk, J. J.; Li, X. Carbon Monoxide Poisoning of Proton Exchange Membrane Fuel Cells. In *International Journal of Energy Research*; 2001; Vol. 25, pp. 695–713.
(19) Cheng, X.; Shi, Z.; Glass, N.; Zhang, L.; Zhang, J.; Song, D.; Liu, Z. S.; Wang, H.; Shen, J. A Review of PEM Hydrogen Fuel Cell Contamination: Impacts, Mechanisms, and Mitigation. *J. Power Sources* **2007**, *165*, 739–756.
(20) Mavrikakis, M.; Barteau, M. A. Oxygenate Reaction Pathways on Transition Metal Surfaces. *J. Mol. Catal. A Chem.* **1998**, *131*, 135–147.
(21) Wang, C.; Boucher, M.; Yang, M.; Saltsburg, H.; Flytzani-Stephanopoulos, M. ZnO-Modified Zirconia as Gold Catalyst Support for the Low-Temperature Methanol Steam Reforming Reaction. *Appl. Catal. B Environ.* **2014**, *154–155*, 142–152.
(22) Cao, S.; Yang, M.; Elnabawy, A. O.; Trimpalis, A.; Wang, C. Inorganometallic Mononuclear Gold Oxo-Clusters Made in Alkaline Solutions as Stable and Selective Catalysts for Methanol Coupling Reactions. *Science.* **2018**, in revision.
(23) Zhai, Y.; Pierre, D.; Si, R.; Deng, W.; Ferrin, P.; Nilekar, A. U.; Peng, G.; Herron, J. A.; Bell, D. C.; Saltsburg, H.; *et al.* Alkali-Stabilized Pt-OHx Species Catalyze Low-Temperature Water-Gas Shift Reactions. *Science.* **2010**, *329*, 1633–1636.
(24) Yang, M.; Li, S.; Wang, Y.; Herron, J. A.; Xu, Y.; Allard, L. F.; Lee, S.; Huang, J.; Mavrikakis, M.; Flytzani-Stephanopoulos, M. Catalytically Active Au-O(OH)x-Species Stabilized by Alkali Ions on Zeolites and Mesoprous Oxides. *Science.* **2014**, *346*, 1498–1501.
(25) Zugic, B.; Bell, D. C.; Flytzani-Stephanopoulos, M. Activation of Carbon-Supported Platinum Catalysts by Sodium for the Low-Temperature Water-Gas Shift Reaction. *Appl. Catal. B Environ.* **2014**, *144*, 243–251.
(26) Zugic, B.; Zhang, S.; Bell, D. C.; Tao, F.; Flytzani-Stephanopoulos, M. Probing the Low-Temperature Water-Gas Shift Activity of Alkali-Promoted Platinum Catalysts Stabilized on Carbon Supports. *J. Am. Chem. Soc.* **2014**, *136*, 3238–3245.
(27) Yang, M.; Liu, J.; Lee, S.; Zugic, B.; Huang, J.; Allard, L. F.; Flytzani-Stephanopoulos, M. A Common Single-Site Pt(II)-O(OH)x- Species Stabilized by Sodium on "Active" and "Inert" Supports Catalyzes the Water-Gas Shift Reaction. *J. Am. Chem. Soc.* **2015**, *137*, 3470–3473.

(28) Qiao, B.; Wang, A.; Yang, X.; Allard, L. F.; Jiang, Z.; Cui, Y.; Liu, J.; Li, J.; Zhang, T. Single-Atom Catalysis of CO Oxidation Using Pt1/FeOx. *Nat. Chem.* **2011**, *3*, 634–641.
(29) Sattler, J. J. H. B.; Ruiz-Martinez, J.; Santillan-Jimenez, E.; Weckhuysen, B. M. Catalytic Dehydrogenation of Light Alkanes on Metals and Metal Oxides. *Chem. Rev.* **2014**, *114*, 10613–10653.
(30) Alper, J. *The Changing Landscape of Hydrocarbon Feedstocks for Chemical Production: Implications for Catalysis*; 2016.
(31) Guo, X.; Fang, G.; Li, G.; Fan, H.; Yu, L.; Wu, X.; Deng, D.; Wei, M.; Tan, D.; Si, R.; *et al.* Direct, Nonoxidative Conversion of Methane to Ethylene, Aromatics, and Hydrogen. *Science.* **2014**, *344*, 616–619.
(32) Zhao, Z.-J.; Chiu, C.; Gong, J. Molecular Understandings on the Activation of Light Hydrocarbons over Heterogeneous Catalysts. *Chem. Sci.* **2015**, *6*, 4403–4425.
(33) Schweitzer, N. M.; Hu, B.; Das, U.; Kim, H.; Greeley, J.; Curtiss, L. A.; Stair, P. C.; Miller, J. T.; Hock, A. S. Propylene Hydrogenation and Propane Dehydrogenation by a Single-Site Zn^{2+} on Silica Catalyst. *ACS Catal.* **2014**, *4*, 1091–1098.
(34) Taccardi, N.; Grabau, M.; Debuschewitz, J.; Distaso, M.; Brandl, M.; Hock, R.; Maier, F.; Papp, C.; Erhard, J.; Neiss, C.; *et al.* Gallium-Rich Pd-Ga Phases as Supported Liquid Metal Catalysts. *Nat. Chem.* **2017**, *9*, 862–867.
(35) Giannakakis, G.; Trimpalis, A.; Shan, J.; Qi, Z.; Cao, S.; Liu, J.; Ye, J.; Biener, J.; Flytzani-Stephanopoulos, M. NiAu Single Atom Alloys for the Non-Oxidative Dehydrogenation of Ethanol to Acetaldehyde and Hydrogen. *Top. Catal.* **2018**, *61*, 1–12.
(36) Tedsree, K.; Li, T.; Jones, S.; Chan, C. W. A.; Yu, K. M. K.; Bagot, P. A. J.; Marquis, E. A.; Smith, G. D. W.; Tsang, S. C. E. Hydrogen Production from Formic Acid Decomposition at Room Temperature Using a Ag–Pd Core–shell Nanocatalyst. *Nat. Nanotechnol.* **2011**, *6*, 302–307.
(37) Wang, Y. Q.; Liang, W. S.; Geng, C. Y. Coalescence Behavior of Gold Nanoparticles. *Nanoscale Res. Lett.* **2009**, *4*, 684–688.
(38) Mihaylov, M.; Knözinger, H.; Hadjiivanov, K.; Gates, B. C. Characterization of the Oxidation States of Supported Gold Species by IR Spectroscopy of Adsorbed CO. *Chemie-Ingenieur-Technik* **2007**, *79*, 795–806.
(39) Moya, S. F.; Martins, R. L.; Schmal, M. Monodispersed and Nanostructrured Ni/SiO2 Catalyst and Its Activity for Non Oxidative Methane Activation. *Appl. Catal. A Gen.* **2011**, *396*, 159–169.
(40) Poncelet, G.; Centeno, M. A.; Molina, R. Characterization of Reduced α-Alumina-Supported Nickel Catalysts by Spectroscopic and Chemisorption Measurements. *Appl. Catal. A Gen.* **2005**, *288*, 232–242.
(41) Tierney, H. L.; Baber, A. E.; Kitchin, J. R.; Sykes, E. C. H. Hydrogen Dissociation and Spillover on Individual Isolated Palladium Atoms. *Phys. Rev. Lett.* **2009**, *103*, 1–4.
(42) Lucci, F. R.; Darby, M. T.; Mattera, M. F. G.; Ivimey, C. J.; Therrien, A. J.; Michaelides, A.; Stamatakis, M.; Sykes, E. C. H. Controlling Hydrogen Activation, Spillover, and Desorption with Pd-Au Single-Atom Alloys. *J. Phys.*

Chem. Lett. **2016**, *7*, 480–485.

Special recognitions received by the PI and co-PI :

PI:

- **2019** ACS Catalysis Lectureship
- **2018** Member, Chemical Sciences Roundtable (CSR), Board on Chemical Sciences and Technology, National Academies of Sciences, Engineering, & Medicine
- **2017** Panel Lead, DOE/BES Workshop on Basic Research Needs (BRN) for Catalysis for Energy, Washington, DC, May 8-10, 2017
- **2017** Director-at-Large, North American Catalysis Society
- **SUCE 2017**, CRE Session Chair, 9th Sino-US joint conference of Chemical Engineering
- **2017** Plenary Lecturer, IGCES2017- Organized by the Chinese Academy of Engineering
- **2016-2018** NAE Section 3, Peer Committee Member
- **2017** Honorary Professor, Beijing University of Chemical Technology, PRC
- **2016** Carol Tyler Award, IPMI
- **2016** Honorary Professor, Tianjin University, PRC

Co-PI:

- **2019** ACS Catalysis Lectureship
- **2018** Panelist, DOE/BRN, Catalysis for Energy Workshop, Washington, DC
- **2018** Named a 2018 AVS Fellow "For pioneering developments in the field of single-atom alloy catalysis and for advancing the fields of molecular motors, molecular self-assembly, and chiral surface chemistry"

Special recognitions received by students/postdocs:

Jilei Liu, won a AIChE/CRE division travel award, AIChE annual meeting, Nov. 2016

JunJun Shan, Jilei Liu, Mengwei Li, Poster award winners, ISCRE 2016, Minneapolis, MN

Andy Therrien, 3 awards - won the Morton Traum Student Award at the AVS 63rd International Symposium & Exhibition. - November 2016, was awarded the Graduate Student Travel Fund from the Office of the Dean of the Graduate School of Arts and Sciences. - January 2017; and the Outstanding Oral Presentation Award at the 18th Annual Northeast Student Chemistry Research Conference. - April 2016

Alex Schilling elected co-chair of Dynamics and Surfaces GRS 2019. - August 2017

Georgios Giannakakis was invited to present a poster at Gordon Research Seminar and Gordon Research Conference on Catalysis. -June 2018

OUTREACH activities

The NanoCatalysis and Energy Laboratory, directed by Maria Flytzani-Stephanopoulos, regularly trains undergraduates in the synthesis, testing and characterization of nanoscale catalysts for more efficient production of hydrogen and chemicals. This past year, two women ChE undergraduates conducted research in the labs, and both of them were co-authors in two different papers (Sylvia Lustig; Fay Wilson).

Cutting edge undergraduate research*:* Tufts University is renowned for the quality of its undergraduate students. Our research labs have undergraduate researchers working within the groups and regularly publishing. For example, undergraduates in the PI's NanoCatalysis and Energy Lab and the Sykes lab have co-authored over twenty papers in the past several years, six of which as first author, and gone onto successful graduate studies at MIT, Harvard, Stanford, Virginia, Maryland, and Rockefeller.

High school outreach

We have established an annual *Reverse Science Fair* between Tufts University and ~300 Medford High School students (304 students in 2017/18) that aims to promote scientific communication between scientists and the community. Each organization uses its strengths to improve the number, diversity, quality, and enthusiasm for high school students' independent research projects. Specifically, the Fair enables high school students to interact with graduate researchers in the run up to their science project presentations, learn about the scientific method, cutting edge research and become familiar with their own science fair judges. The Reverse Science Fair idea was conceived by Sykes, developed by Mernoff (a Medford High teacher), and is being coordinated and assessed by Karen O'Hagan, Chemistry Outreach and Staff Assistant at Tufts University. Assessment occurs via online surveys for both high school student participants and graduate student presenters. Observations are also recorded during the poster presentation. The results of these surveys are discussed by O'Hagan, Mernoff and Sykes and appropriate changes are made to the next year's event. Furthermore, a full write-up of this event was just published in the *Journal of Chemical Education* 2017. ("A Reverse Science Fair that Connects High School Students with University Researchers" B. Mernoff, A. Aldous, N. A. Wasio, J. Kritzer, E. C. H. Sykes, and K. O'Hagan Journal of Chemical Education 2017, 94, 171-176).

We are also currently generating a set of nanoscience teaching tools for high school teachers freely available via the Sykes group website. The 45-minute presentation and accompanying exercises will be modified and used by Gellman and his students. This wider perspective, coupled with feedback from high school students and teachers will be used to improve the material and make it available to a broader range of scientists pursing similar ventures.

Publications Acknowledging this Grant in 2017-2021

(I) Intellectually led by this grant

M. Yang, M. Flytzani-Stephanopoulos, "Design of single-atom metal catalysts on various supports for the low-temperature water-gas shift reaction", *Catal. Today* **2017**, 298, 216-225

G. Garbarino, C. Wang, I. Valsamakis, S. Chitsazan, P. Riani, E. Finocchio, M. Flytzani-Stephanopoulos, G. Busca, "Acido-basicity of lanthana/alumina catalysts and their activity in ethanol conversion", *App. Catal. B: Environ.*, **2017**, 200, 458-468.

M. Flytzani-Stephanopoulos, "Supported metal catalysts at the single-atom limit - A viewpoint", *Chinese J. Catal.*, **2017**, 38, 1432-1442

A. J. Therrien, A. J. R. Hensley, M. D. Marcinkowski, R. Zhang, F. R. Lucci, B. Coughlin, A. C. Schilling, J. McEwen, E. C. H. Sykes "An Atomic-Scale View of Single-Site Pt Catalysis for Low-Temperature CO Oxidation" *Nature Catalysis* **2018**, 1, 192

A. J. Therrien, K. Groden, A. R. Hensley, A. C. Schilling, R. T. Hannagan, M. D. Marcinkowski, A. Pronschinske, F. R. Lucci, E. C. H. Sykes, J. McEwen "Water Activation by Single Pt Atoms Supported on a Cu2O Thin Film" *Journal of Catalysis* **2018**, 364 166

F. R. Lucci, L. Zhang, T. Thuening, M. B. Uhlman, A. C. Schilling, G. Henkelman, E. C. H. Sykes "The Effect of Single Pd Atoms on the Energetics of Recombinative O2 Desorption from Au(111)" *Surface Science* **2018**, 677 296

A. J. Therrien, A. J. R. Hensley, R. T. Hannagan, A. C. Schilling, M. D. Marcinkowski, A. M. Larson, J. McEwen, E. C. H. Sykes "Surface-Templated Assembly of Molecular Methanol on the Thin Film “29” Cu(111) Surface Oxide" *JPCC* **2019**, 123 2911-2921

G. Garbarino, C. Wang, T. Cavattoni, E. Finocchio, P. Riani, M. Flytzani-Stephanopoulos, G. Busca, "A study of Ni/La-Al2O3 catalysts: A competitive system for CO2 methanation" *App. Catal., B: Environ.*, **2019**, 248, 286-297.

S. Cao, M. Yang, A. O. Elnabawy, A. Trimpalis, S. Li, C. Wang, F. Goltl, Z. Chen, J. Liu, J. Shan, M. Li, T. Haas, K.W. Chapman, S. Lee, L.F. Allard, M. Mavrikakis, M. Flytzani-Stephanopoulos "Single-atom gold oxo-clusters prepared in alkaline solutions catalyse the heterogeneous methanol self-coupling reactions" *Nat. Chem.*, **2019**, 11, 1098-1105

C. Wang, M. Ouyang, M. Li, S. Lee, M. Flytzani-Stephanopoulos "Low-Coordinated Pd Catalysts Supported on $Zn_1Zr_1O_x$ Composite Oxides for Selective Methanol Steam Reforming" *Appl. Catal., A*, **2019**, 580, 81-9

M. Ouyang, S. Cao, S. Yang, M. Li, M. Flytzani-Stephanopoulos "Atomically Dispersed Pd Supported on Zinc Oxide for Selective Nonoxidative Ethanol Dehydrogenation" *Ind. Eng. Chem. Res.*, **2020**, DOI: 10.1021/acs.iecr.9b05202

A. C. Schilling, K Groden, J. P. Simonovis, A. Hunt, R. T. Hannagan, V. Cinar, J. McEwen, E. C. H. Sykes, I. Waluyo "Accelerated Cu2O Reduction by Single Pt Atoms at the Metal-Oxide Interface" *ACS Catalysis* **2020**, 10 4215-4226

S. Cao, Y. Zhao, S. Lee, S. Yang, J. Liu, G. Giannakakis, M. Li, M. Ouyang, D. Wang, E. C. H. Sykes, M. Flytzani-Stephanopoulos "High-loading single Pt atom sites [Pt-O(OH)x] catalyze the CO PROX reaction with high activity and selectivity at mild conditions" *Science Advances* **2020**, 6, eaba3809.

J. Liu, A. J. R. Hensley, G. Giannakakis, A. J. Therrien, A. Sukkar, A. C. Schilling, K. Groden, N. Ulumuddin, R. T. Hannagan, M. Ouyang, M. Flytzani-Stephanopoulos, J. McEwen, E. C. H. Sykes "Developing Single-Site Pt Catalysts for the Preferential Oxidation of CO: A Surface Science and First Principles-Guided Approach" Applied Catalysis B: Environmental **2021**, 284 119716

(II) Jointly funded by this grant and other grants with intellectual leadership by other funding sources

Zhao, Y.; Yang, K. R.; Wang, Z.; Yan, X.; Cao, S.; Ye, Y.; Dong, Q.; Zhang, X.; Thorne, J. E.; Jin, L.; Materna, K. L.; Trimpalis, A.; Bai, H.; Fakra, S. C.; Zhong, X.; Wang, P.; Pan, X.; Guo, J.; Flytzani-Stephanopoulos, M.; Brudvig, G. Q.; Batista, V. S.; Wang D. Stable Iridium Dinuclear Heterogeneous Catalysts Supported on Metal-Oxide Substrate for Solar Water Oxidation. *Proc. Natl. Acad. Sci.* **2018**, 201722137

M. D. Marcinkowski, M. T. Darby, J. Liu, J. M. Wimble, F. R. Lucci, S. Lee, A. Michaelides, M. Flytzani-Stephanopoulos, M. Stamatakis, E. C. H. Sykes, "Pt/Cu single-atom alloys as coke-resistant catalysts for efficient C–H activation", *Nat. Chem.*, **2018**, 10, 325-332

Y. Zhao, X. Xan, K. R. Yang, S. Cao, Q. Dong, J. E. Thorne, K. L. Materna, S. Zhu, X. Pan, M. Flytzani-Stephanopoulos, G. W. Brudvig, V. S. Batista, D. Wang, "End-On Bound Iridium Dinuclear Heterogeneous Catalysts on WO3 for Solar Water Oxidation" *ACS Cent. Sci.*, **2018**, 4, 9, 1166-1172.